 MCB, vol.11, no.4, pp.221-234, 2014

Fluid Structure Modelling of Blood Flow in Vessels

M. Moatamedi*, M. Souli† and E. Al-Bahkali‡

Abstract: This paper describes the capabilities of fluid structure interaction based multi-physics numerical modelling in solving problems related to vascular biomechanics. In this research work, the onset of a pressure pulse was simulated at the entrance of a three dimensional straight segment of the blood vessel like circular tube and the resulting dynamic response in the form of a propagating pulse wave through the wall was analysed and compared. Good agreement was found between the numerical results and the theoretical description of an idealized artery. Work has also been done on implementing the material constitutive models specific for vascular applications.

Keywords: Multi-physics, Blood vessels, Fluid structure interaction, ALE.

1 Introduction

The study of the cardiovascular system dates back all the way to the beginning of medical science with Hippocrates and Aristotle taking interest in the topic. Since then the importance of the heart and blood vessels has developed into a science in itself. According to the World Health Organisation (WHO) in 2002, alone there were 16.7 million deaths globally related to various forms of cardiovascular diseases (CVD) [1]. A large proportion of these cardiovascular diseases find their origins in the blood vessels. Recently, interest in blood vessels has extended from purely disease related topics to other issues such as blunt traumatic aorta rupture (BTAR), which may occur in circumstances such as automotive accidents [2,3]. Although the incidence of such deaths is relatively low, but it is gaining interest as it is something that can be avoided by increased understanding of the biomechanics of the problem.

It is regarded that the progression of most vascular diseases is influenced by a complex interaction of the biochemical and biomechanical factors. The exact mech-

* Narvik University College, Narvik, Norway.
† Université de Lille1, LML, UMR CNRS 8107, France.
‡ College of Engineering , King Saud University, Saudi Arabia.

anisms of most of these diseases remain uncertain and are currently being extensively studied. In recent years strong links between mechanical conditions in vessels and certain diseases have been established. High nonlinearities associated with the behaviour of blood vessels in the human body limit the practical application of the analytical methods in their evaluation. Accurate measurement of mechanical parameters in vivo using experimental methods is extremely difficult, if not impossible. Much progress has been made using medical imaging equipment, however challenges still remains. These factors have opened the door to numerical simulations, which are able to give acceptable predictions of the mechanical behaviour of blood vessels based on the minimal input information.

Numerical simulations are increasingly being used in all branches of the biomechanics and provide valuable information to understand the basic physics of various parts of the human anatomy. Computational fluid dynamics has extensively been applied to examine the flow behaviour of blood through various parts of the cardiovascular system. These simulations are gradually expanded to include results for the wall shear stress distributions of the blood vessels [4]. Design and optimization of medical devices and cardiovascular implants such as stents has been studied using finite elements based multi-physics numerical techniques [5].

Blood vessels are highly elastic in behaviour. The influence of pulsating blood flow is substantial on vessel walls. In many cases the approach of considering the flow and structural responses independent of each other becomes insufficient and use of fluid structure interaction becomes a necessity. Analytical solutions of fluid-structure interaction problems related to the blood vessel have been around for many years now. Moens [6] examined the propagation of flow vibrations on elastic tube and Womersly investigated the dynamic response of an elastic tube with a sinusoidal flow and defined an analytical solution for the flow field. Now the availability of low-cost computing has led to the development of several numerical methods to study the fluid-structure interaction. Most numerical codes of fluid structure interaction were created with having purely engineering applications in mind, such as the study of aero-elastic effects in aircraft or the effect of underwater explosions on submarine hulls, but now a days the fluid-structure interaction simulations have diversified and found a large application in determining the correlation between disease and physical phenomena.

Two types of fluid structure interaction methods are available are used in this apper, Merge node method where the fluid mesh and structure mesh are sharing common nodes at the coupling interface and Penalty method, which consist to a structural Lagrangian mesh embedded into an ALE fluid mesh. For this research work the fully coupled penalty method is employed, where the Lagrangian mesh moves through the Eulerian mesh and interface springs are placed between penetrating

nodes and the contact surface. Material models for use in biomechanics are, in general, poorly catered for in commercial finite element codes. When desiring a more accurate representation than that given by a linear elastic material model, the user usually has to satisfy themselves with using a standard hyper-elastic or viscoelastic model. Such models are usually insufficient for describing composite soft biological tissue in its physiological state. If a more accurate model is desired by the user, it has to be implemented through a user-subroutine. This paper also describes that how such a user defined model can be implemented in any code development see [7] and [8].

2 Theory and Mathematical Description

2.1 ALE and Eulerian Formulation for the Fluid

Fluid problems, where interfaces between different materials such as air and water, or, air and blood exist can easily modelled by using a Lagrangian mesh. However for complex geometry, the distortion of the Lagrangian mesh makes this technique difficult as many re-meshing steps are required for the calculation to continue. An alternative method to use is the Eulerian or ALE formulation. This method introduces two problems. The first problem is the interface tracking and the second problem is the advection phase or advection of fluid material across element boundaries. To solve these problems, an explicit finite element method for the Lagrangian phase and a finite volume method (flux method) for the advection phase are used. We can refer to several explicit codes such LS-DYNA see [9] for a full description of the explicit finite element method and ALE mesh motion.

An ALE formulation contains both pure Lagrangian and pure Eulerian formulations. The pure Lagrangian description is the approach where the mesh moves with the material, making it easy to track interfaces and apply boundary conditions. Using an Eulerian description, the mesh remains fixed while the material passes through it. Interfaces and boundary conditions are difficult to track using this approach; however, mesh distortion is not a problem because the mesh never changes. In order to simplify the equations a relative velocity $w = v - u$ is introduced, where v is the fluid velocity and u the domain or mesh velocity. The governing equations for the ALE formulation are given by the following conservation equations:

Mass Equation

$$\frac{\partial \rho}{\partial t} = -\rho \frac{\partial v_i}{\partial x_i} - w_i \frac{\partial \rho}{\partial x_i} \tag{1}$$

Momentum Equation

The strong form of the problem governing Newtonian fluid flow in a fixed domain

consists of the governing equations and suitable initial and boundary conditions. The equations governing the fluid problem are the ALE description of the Navier-Stokes equations:

$$\rho \frac{\partial v_i}{\partial t} = \sigma_{ij,j} + \rho b_i - \rho w_i \frac{\partial v_i}{\partial x_j} \tag{2}$$

The stress tensor σ_{ij} is described as follows:

$$\sigma_{ij} = -p\delta_{ij} + \mu(v_{i,j} + v_{j,i}). \tag{3}$$

where n_i is the outward unit normal vector on the boundary, and δ_{ij} is Kronecker's delta function.

Energy Equation

$$\rho \frac{\partial E}{\partial t} = \sigma_{ij} v_{i,j} + \rho b_i v_i - \rho w_j \frac{\partial E}{\partial x_j} \tag{4}$$

Eulerian equations commonly used in fluid mechanics by the CFD community are derived by assuming that the velocity of the reference configuration is zero and that the relative velocity between the material and the reference configuration is therefore the material velocity. The term in the relative velocity in equation 3 and 4 is usually referred to as the adjective term, and accounts for the transport of the material past the mesh. It is the additional term in the equations that makes solving the ALE equations much more difficult numerically than the Lagrangian equations, where the relative velocity is zero. There are two ways to implement the ALE equations and they correspond to the two approaches taken in implementing the Eulerian viewpoint in fluid mechanics. The first way solves the fully coupled equations for computational fluid mechanics; this approach used by different authors can handle only a single material in an element. The alternative approach is referred to as an operator split in the literature, where the calculation, for each time step is divided into two phases.

First a Lagrangian phase is performed where the mesh moves with the material. In this phase the changes in velocity and internal energy due to the internal and external forces are calculated. The equilibrium equations to be discretised and solved are:

$$\rho \frac{\partial v_i}{\partial t} = \sigma_{ij,j} + \rho b_i, \tag{5}$$

$$\rho \frac{\partial E}{\partial t} = \sigma_{ij} v_{i,j} + \rho b_i v_i. \tag{6}$$

In the Lagrangian phase, mass is automatically conserved, since no material flows across element boundaries. In second phase an advection phase is performed, where the transport of mass, momentum and internal energy across the element boundaries is computed. This phase may be considered as remapping phase. The displaced mesh from the Lagrangian phase is remapped into the initial mesh for an Eulerian formulation, or an arbitrary distorted mesh for an ALE formulation.

2.2 Coupling algorithm

The detailed description of finite element contact algorithms is not the goal of this paper. However, since the coupling method described in this paper is based on the penalty method for contact algorithms, the contact approach is a good introduction to this method. In contact algorithms, a contact force is computed proportional to the penetration vector, the amount the constraint is violated. In an explicit FEM method, contact algorithms compute interface forces due to impact of the structure on the fluid; these forces are applied to the fluid and structure nodes in contact in order to prevent a node from passing through contact interface. An ALE or Lagrangian mesh is used for the fluid. The literature on contact algorithms is extensive, but most of it is devoted to static problems. The literature devoted to contact for dynamic fluid structure interaction problems is very limited: one of the problems encountered in these applications is the high mesh distortion at the contact interface due to high fluid nodal displacement and velocity.

This problem is still unsolved since most of the ALE re-meshing algorithms including the equipotential method are not efficient to maintain a regular mesh for the calculation to continue. In contact algorithms one surface is designated as a slave surface, and the second as a master surface. The nodes lying on both surfaces are also called slave and master nodes respectively. For a fluid structure coupling problem, for example fluid with an initial velocity impacting a structure, as described in [10], the fluid nodes at the interface are considered as slave, and the structure elements as master. The first approach for contact is the kinematic contact, constraining fluid and structure nodes to the same velocity. Kinematic contact conserves total momentum, but not total energy. The second approach, the penalty contact, is different from the previous one. The penalty method imposes a resisting force to the slave node, proportional to the penetration through the master segment. This force is applied to both the slave node and the nodes of the master segment in opposite direction to satisfy equilibrium forces.

$$\vec{F}_s = k.\vec{d} \quad \text{and} \quad \vec{F}_f = -\vec{F}_s \tag{7}$$

The coupling technique described in figure 1 is based on penalty contact algorithm used in structure mechanics, where a contact interface defined though the mesh sep-

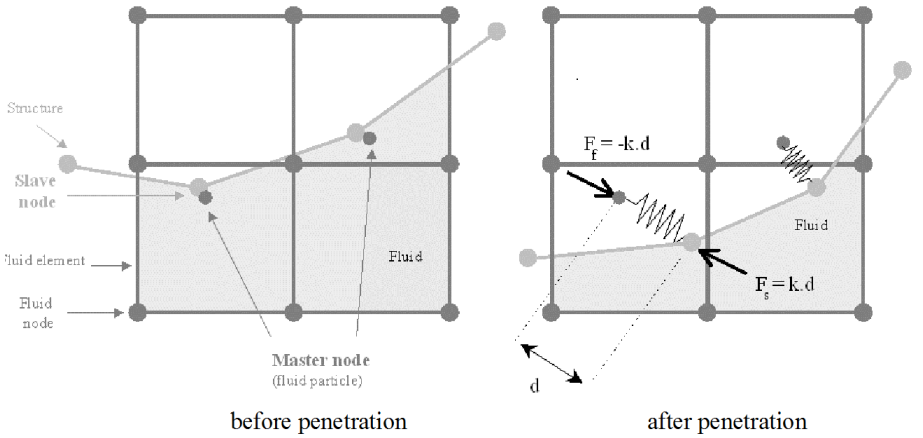

Figure 1: Coupling algorithm before and after penetration.

arates the fluid mesh from the structure mesh. Thus contact forces applied from the fluid to the structure and conversely. In contact a master node is represented trough a fluid node whereas in coupling the master node is a fluid particle represented through its local coordinates in the fluid element.

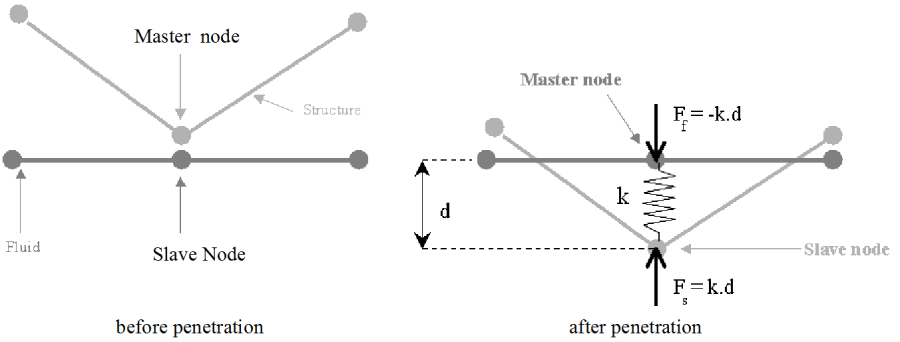

Figure 2: Contact algorithm before and after penetration.

3 Numerical Setup

Numerical setup used for this three dimensional fluid structure interaction study was based on a tube of 80mm length with an internal diameter of 4mm and a wall thickness of 0.12mm. The vessel wall was described as linearly elastic with a

density of 1075kg/m^3, a Poisson's ratio of 0.45 and an initial Young's modulus of 3MPa, values representative of blood vessels in the physiological state. The fluid domain is defined as an incompressible Newtonian model of water, a realistic assumption for modelling the blood. A density of 1000kg/m^3 and a viscosity of 0.001Pa.s were therefore chosen. The problem was set-up in LS-DYNA with 68,480 elements describing the fluid domain, while the blood vessel wall was discretised using 4848 Belythchko-Tsay elements. Constraints were applied on the vessel wall at the inlet section on translation in the direction of flow and in all translational degrees of freedom at the exit. The onset of a sinusoidal pressure wave was simulated at the vessel entrance by a linearly increasing pressure from zero to 352Pa over a time period of 10ms.

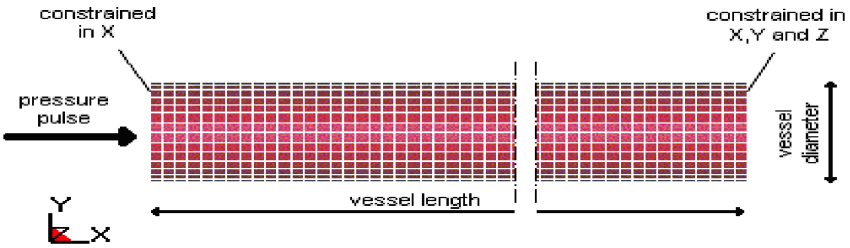

Figure 3: Boundary Conditions.

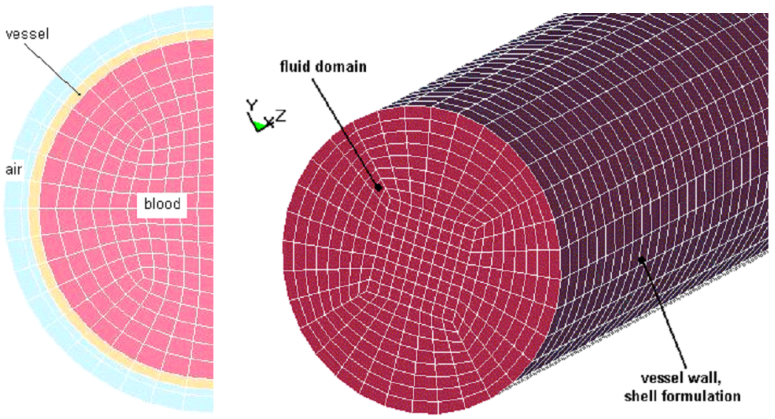

Figure 4: Computational Mesh (Penalty Method).

3.1 Numerical Validation

Performance of the fluid structure interaction related calculations of LS-DYNA was evaluated by analysing the Moens-Korteweg wave speed described by Kuntz and Menter [11]. The pressure pulse down the vessel wall is known as the wave speed. The wave speed is highly dependent on the elastic behavior of the blood vessel wall. The blood vessel was described as an elastic tube through which the blood ejected by the heart, flows in the form of pressure and flow waves. The wave propagates through the tube in the form of a radial displacement of the blood vessel wall. Assuming blood as an in-viscid and incompressible fluid, flowing through a thin vessel constrained in the direction of the flow; the Moens-Korteweg equation [6] gives the resulting wave speed (c_o):

$$c_0 = \sqrt{\frac{E.h}{2R.\rho}} \tag{8}$$

Where, E is the Young's Modulus of a pipe of internal radius R, with a wall thickness t, carrying a fluid of density ρ. Errors caused as a result of assuming a thin tube in (1) can be estimated by using the Bergel correction [12], which accounts for the thickness through Poisson's ratio (υ). The difference between the two is given as:

$$\left(\frac{c'}{c_0}\right)^2 = \frac{(2-\gamma)}{[2-2\gamma(1-v-2v^2)+\gamma^2(1-v-2v^2)-2v^2]} \tag{9}$$

Where, γ is the ratio of wall thickness and tube outer radius. Simplifying this expression and incorporating it into equation (1), the wave speed (c') becomes:

$$c' = \sqrt{\frac{E.h}{2R.\rho(1-v^2)}} \tag{10}$$

Figure 5 shows the numerical results of pressure wave propagation along the test tube at different time intervals. As pressure wave moves along the tube, the diameter of tube gets change. The wave speed can be estimated by measuring the progression of the radial displacement at number of locations along the tube over time.

A comparison was made between numerical results and Moens-Korteweg theory by varying the Young's modulus. Radial displacement results at different locations along the tube were extracted at 1ms time intervals from LS-DYNA and the wave speed was evaluated from these by sub-routines written in MATLAB (MathWorks, Natick, MA, USA).

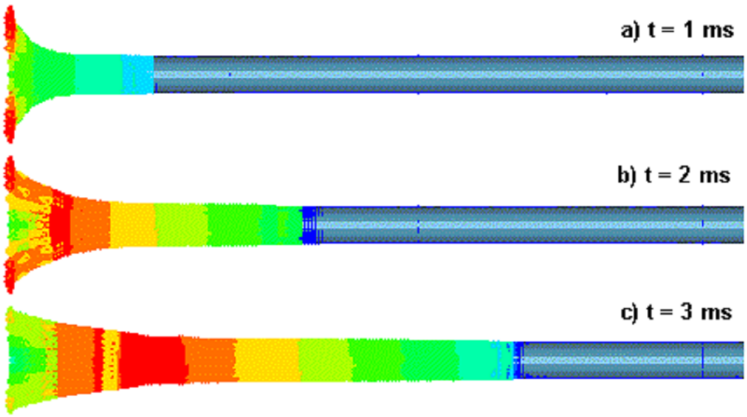

Figure 5: Propagation of pressure wave along tube at different time intervals.

When using the realistic value for water wave speed of 1465m/s, the time step became extremely small and leads to high computational time. Considering that the time over which the current simulation is run for is 10ms, the prospect of running a full cardiac cycle with a length of 1s, which is planned for future research, would become prohibitive and inefficient in computational terms. Therefore, it was decided to dramatically scale down this parameter. Initially a very low value of 15m/s was selected. Varying the speed of sound in a separate study, it was found that displacement results converged at a value of 60m/s, a value that maintains the practicality of solving vascular biomechanics problems of this nature. Using a Pentium-IV PC running at 3 GHz with a random access memory of 1GB, the computational time was just over 2 hours, significantly higher than the time required when the model was run at a fluid speed of sound of 15m/s. Figure 4 shows the numerical results obtained for the pulse wave speed, as from the current model in LS-DYNA, as a function of Young's modulus, with a comparison with the works done by Moens-Korteweg (Eq. 10) [6] .()(Leiden 1878) and Kuntz and Menter [11].

4 Vascular Material Models

The dynamic behaviour of blood vessels suggests them as non-linear structures because they exhibit hysteresis, relaxation and creep, all characteristics of viscoelasticity. The properties vary depending on proximity to the heart, age, individual variation and health issues amongst other factors. Obtaining material properties for use with numerical simulations can be complex and many researchers have experi-

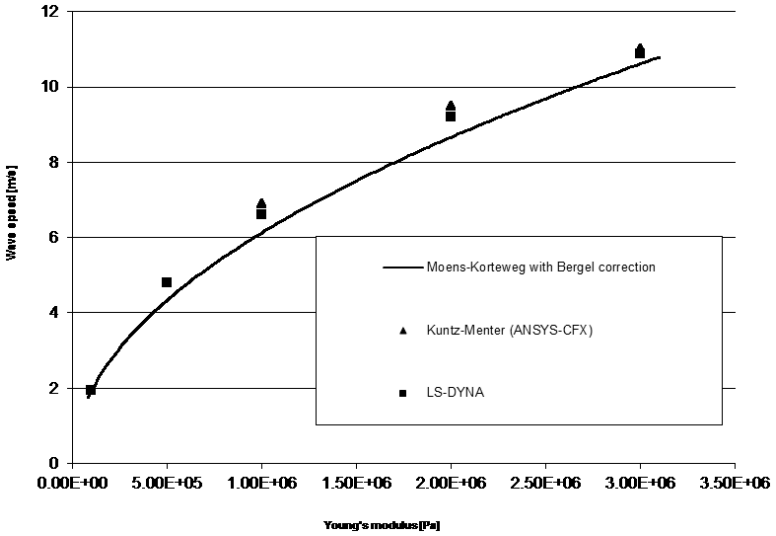

Figure 6: Wave speed as function of Young's modulus: Comparison of numerical results and idealised theory.

enced difficulty in obtaining appropriate wall mechanics data for their models. The usual method of obtaining the necessary data for material is by performing uniaxial stress-strain tests on in vitro blood vessel segments. Many researchers had opted for the more complex multi-axial experiments under the argument that these can give the full tensorial relationship. However, even the simplest uni-axial tests can be difficult to perform and require a degree of experience as well as specialised equipment capable of acquiring the data.

A range of elastic, hyper-elastic and viscoelastic constitutive models have been proposed for representing various soft tissues. The predominant form in literature seems to be under the assumption of hyper-elasticity, i.e. described in the form of a strain energy density function. Strain energy density functions are convenient as they provide a direct relationship between the strain parameters and resulting stresses. One of the most popular constitutive models for describing soft tissue was introduced by Fung [13]. This model is expressed as an exponential form strain energy density function.

$$\psi = \frac{\mu}{2b}\left[\exp\left(b\left(I_1 - 3\right)\right) - 1\right] \tag{11}$$

Where, μ is the shear modulus, b is a positive material constant, I_1 is the first invariant of the right Cauchy-Green stress tensor and is defined as $I_1 = tr(C)$. The

right Cauchy-Green tensor can be obtained from the deformation gradient matrix:

$$C = F^T F \tag{12}$$

Another common way to express strain energy density functions is through various forms of the standard neo-Hookean model:

$$\psi = \frac{\mu}{2}(I_1 - 3) \tag{13}$$

Biological tissues are made up of cells, extra cellular matrices and large amounts of water lodged in between. The extra cellular matrices are made up of fibres, such as the proteins elastin and collagen, and a ground substance. A blood vessel is no different and is composed of three main layers; the intima, media and adventitia. Each of these has a different composition of the basic building blocks as well as fibre orientations. As a result we have three very different layers in terms of mechanical behaviour which have to be treated differently to a certain extent.

4.1 Holzapfel Material Model

Holzapfel [14] presented a constitutive model for modelling the mechanical response of individual arterial layers along with a method of extracting the necessary data from quasi-static uniaxial extension tests. The underlying assumptions of this model are that the structure is that of an isotropic ground matrix with two embedded families of collagen fibres and is of homogenous composition. The Holzapfel model is based on a strain-energy function which accounts for the isotropic (ψ_{ISO}) and orthotropic (ψ_{ORTHO}) contributions of the artery material individually. The strain energy function is expressed in terms of Green-Lagrange strains in the circumferential (E_{11}) and axial directions (E_{22}):

$$\hat{\psi} = \hat{\psi}_{ISO}(E_{11}, E_{22}) + \hat{\psi}_{ORTHO}(E_{11}, E_{22}) \tag{14}$$

The isotropic contribution assumes the form of a standard neo-Hookean material and is defined as:

$$\hat{\psi}_{ISO}(E_{11}, E_{22}) = \frac{\mu}{2}\left\{2(E_{11} + E_{22}) + [(2E_{11} + 1)(2E_{22} + 1)]^{-1} - 1\right\} \tag{15}$$

The orthotropic contribution is expressed as a Fung-type function:

$$\hat{\psi}_{ORTHO}(E_{11}, E_{22}) = C[\exp(Q) - 1] \tag{16}$$

Where Q is defined as:

$$Q = c_{11}E_{11}^2 + c_{12}E_{11}E_{22} + c_{22}E_{22}^2 \tag{17}$$

Where, C is a stress like parameter and c11, c22 and c12 are non-dimensional material parameters, all obtained by experiment. The circumferential and axial components of the second Piola-Kirchoff stress tensor can be fund simply:

$$S_{11} = \frac{\partial \hat{\psi}(E_{11}, E_{22})}{\partial E_{11}} \tag{18}$$

$$S_{22} = \frac{\partial \hat{\psi}(E_{11}, E_{22})}{\partial E_{22}} \tag{19}$$

Noting that S_{33} was assumed to be zero during the derivation, as can be seen, the model is two-dimensional in formulation; however Holzapfel points out that it is inherently 3D for isochoric deformations without shearing. Since the model does not include shear stresses its usage is limited to simple stress-strain tests and axisymmetric pressure loadings. These constitutive equations have been implanted into material user subroutine in LS-DYNA and tested by a single element validation.

4.2 Implementing Holzapfel constitutive material models.

The validation study is based on a single cube element 1mm in dimension. A constant displacement was applied to nodes on opposite sides of the element in the positive and negative x direction. The validation was performed using material data for the tunica intima and tunica media as published by [14,15]. Numerical results of the strains in the circumferential and axial directions were compared with experimental data. Numerical strain predictions were seen to be reliable. Results for the intima layer closely followed experimental values (Figure 7) , while some differences are seen between the two sets of results for the media.

5 Conclusion

The implementation of fluid-structure interaction methods for blood vessel applications has been investigated in this research work. Much effort was invested to setup and validate the numerical simulations for use in research linked to blunt traumatic aortic rupture. Good agreement was found between the numerical results and the theoretical description of an idealized artery. A material constitutive model for blood vessels has also been implemented in LS-DYNA in an attempt to improve the quality of numerical simulations and better understanding of flow in blood vessels. Numerical simulations from ALE and FSI methods can be included in shape design optimization with shape optimal design techniques, see [16], and material optimisation, see [17,18]. Once simulations are validated by test results, they can be used as design tool for the improvement of the system structure being involved.

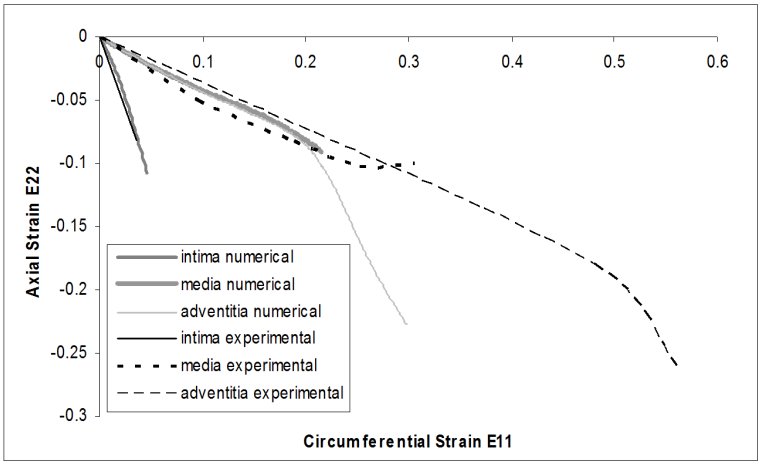

Figure 7: Circumferential strain versus axial strain for LS-DYNA numerical results and experimental results.

Acknowledgement: The authors would like to acknowledge contribution of A. Zhao of AZ Engineering & Science, USA.

References

1. Mackay, J. & M. G. (2004) Atlas of Heart Diseases and Stroke, World Health Organisation Press.

2. Richens, D., Field, M. et al. (2004) A finite element model of blunt traumatic aortic rupture. *European Journal of Cardio-thoracic Surgery,* 25, 1039-1047.

3. Pericevic, I. & M. M. (2007) Application of the penalty coupling method for the analysis of blood vessels. *European Journal of Computational Mechanics,* 16, (2), 537-548.

4. Gijsen, F. J. H., Van de Vosse, F. N. et al. (1999) The influence of the non-Newtonian properties of blood on the flow large arteries: steady flow in a carotid bifurcation model. *Journal of Biomechanics,* 32, 601-608.

5. Migliavacca, F., Petrini, L. et al. (2005) A predictive study of the mechanical behaviour of coronary stents by computer modelling. *Medical Engineering & Physics*, 27, 13-18.

6. Leiden, M. A. D. P. (1878) The Netherlands: E.J. Brill. OCLC (1878).

7. Aquelet, N., Souli, M., Olovson, L. (2006) Euler Lagrange coupling with damping effects: Application to slamming problems. *Computer Methods in Applied Mechanics and Engineering,* 195, 110- 132, 2006.

8. Khan, M. U., Moatamedi, M., Souli, M. (2008) Multiphysics out of position airbag simulation I. *nternational Journal of Crashwortiness,* 13, 159-166.

9. Hallquist, J. O. (1998) LS_DYNA Theory Manual, *Livermore: Livermore Software Technology Corporation (1998).*

10. Longatte, E., Verreman, V. et al. (2009) Time marching for simulation of Fluid-Structure Interaction Problems. *Journal of Fluids and Structures,* 25, (1), 95-111.

11. Kuntz, M. & M. FR (2004) Simulation of fluid-structure interactions in aeronautical applications. European Congress on Computational Methods in Applied Sciences and Engineering.

12. Messahel, R., Cohen, B., Souli, M., Moatamedi, M. (2011) Fluid-structure interaction for water hammers effects in petroleum and nuclear plants. *The International Journal of Multiphysics,* 5, 377-386.

13. YCB, F. (1967) Elasticity of soft tissues in simple elongation. *Am J Physiol,* 213, 1532-1544.

14. Holzapfel, G. A. (2006) Determination of material models for arterial walls from uniaxial extension tests and histological structure. *Journal of Theoretical Biology,* 238, 290-302.

15. Al-Bahkali, E., Erchiqui, F., Souli, M., Moatamedi, M. (2013) Deployment of a Neo-Hookean membrane: experimental and numerical analysis . *The International Journal of Multiphysics,* 7, 41-51.

16. Souli, M. & Zolesio, J. P. (1993) Shape Derivative of Discretized Problems. *Computer Methods in Applied Mechanics and Engineering,* 108, 187–199.

17. Erchiqui, F., Souli, M. & Ben Yedder R. (2007) Non isothermal finite-element analysis of thermoforming of polyethylene terephthalate sheet: Incomplete effect of the forming stage. *Polymer Engineering and Science,* 47, 12, 2129-2144.

18. Barras, G., Souli, M., Aquelet, N. & Couty, N. (2012) Numerical simulation of underwater explosions using an ALE method. The pulsating bubble phenomena. *Ocean Engineering, an international Journal,* 41, 53–66.